Effects of the surroundings and conformerisation of *n*-dodecane molecules on evaporation/condensation processes

Vladimir M. Gun'ko

Chuiko Institute of Surface Chemistry, 17 General Naumov Street, Kiev 03164, Ukraine and
Sir Harry Ricardo Laboratories, School of Computing, Engineering and Mathematics, University of Brighton,
Cockcroft Building, Lewes Road, Brighton BN2 4GJ, United Kingdom

Rasoul Nasiri and Sergei S. Sazhin [a]

Sir Harry Ricardo Laboratories, School of Computing, Engineering and Mathematics, University of Brighton,
Cockcroft Building, Lewes Road, Brighton BN2 4GJ, United Kingdom

The evaporation/condensation coefficient (β) and the evaporation rate (γ) for *n*-dodecane *vs.* temperature, gas pressure, gas and liquid density, and solvation effects at a droplet surface are analysed using quantum chemical DFT calculations of several ensembles of conformers of *n*-dodecane molecules in the gas phase (hybrid functional ωB97X-D with the cc-pVTZ and cc-pVDZ basis sets) and in liquid phase (solvation method SMD/ωB97X-D). It is shown that β depends more strongly on a number of neighbouring molecules interacting with an evaporating molecule at a droplet surface (this number is estimated through changes in the surface Gibbs free energy of solvation) than on pressure in the gas phase or conformerisation and cross-conformerisation of molecules in both phases. Thus, temperature and the surrounding effects at droplet surfaces are the dominant factors affecting the values of β for *n*-dodecane molecules. These values are shown to be similar (at reduced temperatures $T/T_c < 0.8$) or slightly larger (at $T/T_c > 0.8$) than the values of β calculated by the MD FF methods. This endorses the reliability of the previously developed classical approach to estimation of β by the MD FF methods, except at temperatures close to the critical temperature.

[a] E-mail address: S.Sazhin@brighton.ac.uk

I. INTRODUCTION

Processes of the evaporation of liquids and condensation of vapours play important roles in nature, agriculture, industry, and medicine.[1-6] These processes have various features in huge (*e.g.* oceans, seas, lakes, rivers, and soils) and relatively small (sprays, Diesel engines, droplets sessile at a flat surface or located in porous media) systems.[4-39] The evaporation/condensation processes depend strongly on ambient conditions (temperature, pressure, free or restricted volumes of liquid and gas, droplet sizes, gas flow rate and level of turbulence) and types of evaporating/condensing compounds (sizes, structure, and polarity of molecules, mixture composition of liquids, presence and type of solutes).[2-15] The type of compound determines the characteristics of intermolecular interactions in liquids affecting the rates of evaporation and condensation depending on a number of parameters, including temperature, and total and partial gas (vapour) pressures.[2,3,5-15] Our analysis is focused on *n*-alkane droplets with predominant van-der-Waals (vdW) intermolecular interactions. The approach developed in this paper, however, is relatively general and can be applied to both small and large systems with nonpolar or polar compounds since it is focused mainly on the changes in the Gibbs free energy occurring due to transfer of a molecule from a liquid surface to the gas phase during evaporation and *vice versa* during condensation at various temperatures and pressures.

The evaporation and condensation of droplets have been studied using both experimental methods and theoretical modelling based on hydrodynamic and kinetic approaches.[5-15] Two parameters, the evaporation/condensation coefficient (β) and the evaporation rate (γ), have been used to describe these processes. The evaporation rate, γ, was considered in a number of papers based on quantum chemical (QC) methods.[38-41] It was studied for *n*-alkane molecules in the C_8-C_{27} range for molecular clusters and nanodroplets.[40,41] The analysis was based on the QC solvation (SMD) method and the kinetic gas theory, assuming that the system is in a state of thermodynamic equilibrium, *i.e.* the evaporation and condensation rates are equal. The kinetic gas theory was applied to estimate the

collision rate of molecules/clusters/nanodroplets in the gas phase. An increase in the molecular size of evaporating alkanes resulted in a strong decrease in the values of γ.

The evaporation/condensation coefficient, β, is particularly important for kinetic modelling, where it is used for formulation of the kinetic boundary conditions at the surface of the droplet.[6,8] There are several theoretical methods and techniques used to estimate the values of β *vs*. temperature, total and partial pressures, and liquid/gas/vapour composition. In the molecular dynamics (MD) approach[6,8,35-37], interactions between individual molecules are described by the non-reactive or reactive force fields (FF) or quantum chemical methods. *Ab initio*, density functional theory (DFT), and semiempirical QC methods are used alongside MD, trajectory, dynamic reaction coordinate, and other techniques.[38-41] It was shown that the QC *ab initio* and DFT methods with appropriate basis sets lead to more accurate modelling of the evaporation and condensation processes than semiempirical or MD FF methods. However, QC *ab initio* and DFT methods require much longer computation time for much smaller droplets (clusters or nanodroplets) than MD FF. These two approaches are essentially complementary and the comparison between them can be used to justify the range of applicability of classical MD FF.

The intermolecular bonds in droplets with nonpolar or weakly polar organics (*e.g.* normal, iso- and cycloalkanes, and aromatics) are of the vdW type[42] characterised by relatively weak short-range forces (permanent dipole − permanent dipole, permanent dipole − induced dipole, and transitory dipole − transitory dipole interactions) controlling the behaviour of Lennard-Jones (LJ) fluids.[43,44] The vdW type of intermolecular interactions allow one to simplify the modelling using the molecular mechanics (MM) and MD methods with various vdW and LJ FF.[6,8,13-15] The models were applied to both individual liquids and complex mixtures including a number of compounds which can be evaporated under various conditions.[43-51] The reliability and the accuracy of MD FF approaches to modelling the temperature/pressure behaviour of liquid droplets and determination of the functions

$\beta(T)$ and $\gamma(T)$ under various conditions, however, still needs to be investigated. The present work is focused on the analysis of β as a function of temperature, pressure, gas and liquid density, and surface surrounding effects affecting the interaction of evaporating molecules with neighbouring molecules. The analysis is based on the transition state theory (TST) and quantum chemical DFT methods applied to several ensembles of conformers of n-dodecane molecules. In contrast to the previous studies,[6,8] in this paper the TST is based on a more accurate QC DFT approach taking into account the conformerisation of n-dodecane molecules. As in the previous studies (*e.g.*[41]), n-dodecane is considered as a representative of n-alkanes in Diesel fuel. The results are compared with the values of β previously computed using the MD FF methods.[6,8,13-15,36,37,52]

II.   COMPUTATION METHODS

Quantum chemical (QC) calculations were carried out using the density functional theory (DFT) method with a hybrid functional ωB97X-D[53-55] (labelled as wB97XD in Gaussian 09) and two (cc-pVTZ (larger) and cc-pVDZ (smaller)) basis sets with the Gaussian 09 program suite.[53] The geometry of n-dodecane conformers was optimised using ωB97X-D/cc-pVTZ. All calculations were performed taking into account zero-point and thermal (calculating vibrational spectra) corrections to the Gibbs free energy of each conformer of n-dodecane. The solvation effects for n-dodecane conformers in n-dodecane medium were analysed based on the application of the solvation method SMD[56] implemented in Gaussian 09. This allowed us to compute the Gibbs free energy of solvation, $\Delta G_s = G_l - G_g$, where G_l and G_g are the Gibbs free energies of a molecule in the liquid and gas media, respectively.

Functional ωB97X-D, used in our analysis, introduces empirical damped atom-pairwise dispersion terms into the functional containing range-separated Hartree-Fock exchange for improved description of the vdW interactions.[53-57] Therefore this functional was selected to obtain more

adequate results for n-dodecane conformers in the gas and liquid (SMD) phases than those obtained previously using functional B3LYP. [40,41] To analyse the basis set size effects, the calculations were carried out using cc-pVTZ and cc-pVDZ, providing 724 and 298 basis functions for an n-dodecane molecule respectively.

A batch of QC DFT calculations was carried out at various temperatures. Also, the temperature effects were estimated using QC results at $T_0 = 298.15$ K and certain temperature-dependent corrections for $\Delta G_{l \to g}(T) = G_g(T) - G_l(T)$ and $\Delta G_{g \to l}(T)$ (see Supplementary Information (SI)[58]).

For visualisation of the fields around molecules, the TorchLite (version 10.3, 2014) program was used.[59,60] Although all interactions at a molecular level are electrostatic in origin, the whole electrostatic field surrounding the molecule can be split into four types of interactions or fields, which correspond to (i) predominantly hydrophobic interactions, (ii) vdW attraction forces, and electrostatic fields dominated by (iii) electropositive or (iv) electronegative atoms or ions. In the field visualisation approach each atom or group of atoms is considered as a "field point" of one of these four types; all field points give continuous fields.[59,60] For n-alkanes, the first two fields are the dominant. Visualisation of molecular structures was also performed with the help of the ChemCraft (version 1.7/382) program.[61]

Previous QC MD and dynamic reaction coordinate calculations showed[40,41] that linear, flexible, and relatively long (~1.6 nm) n-dodecane molecules can change their conformation in both liquid and gas phases, and these dynamic changes increase and become faster at higher temperatures. Changes in the conformer structures of n-alkanes can easily occur, especially at high temperatures, due to relatively low barriers to the rotations of CH_2 groups around C–C bonds.[43,44] This suggests that the effects of both the conformerisation and cross-conformerisation (changes in conformer state during transfer into another phase) of n-dodecane molecules (CDM) should be considered during calculations of β and γ (see SI[58]).

Several approaches to the definition of the evaporation/condensation coefficient β were used (see SI). Firstly, the averaged condensation coefficient β_g, which is close to the evaporation coefficient for the systems in equilibrium or quasi-equilibrium state, can be estimated in terms of thermodynamic potentials[34,51]

$$\frac{1-\langle\beta_g\rangle}{\langle\beta_g\rangle}=\exp\left(\frac{\langle\Delta G_{v\to l}\rangle}{RT}\right),\tag{1}$$

where $\Delta G_{v\to l}=G_l-G_v$ is the difference between the Gibbs free energies of molecules in a liquid and a vacuum, and averaging is carried out following Eqs. (S1) and (S2) (see SI). The values of $<\beta_g(T)>$ can be corrected using averaged (over a set of conformers) function α_g obtained from the following equation

$$\frac{1-\langle\alpha_g\rangle}{\langle\alpha_g\rangle}=\exp\left(\frac{\langle\Delta G_{l\to v}\rangle}{RT}\right).\tag{2}$$

where $\Delta G_{l\to v}$ is the change in the Gibbs free energy upon transfer of a molecule from liquid state into a vacuum to form the gas phase. The value of $<\alpha_g>$ should be subtracted from $<\beta_g>$ to consider the transfer between gas (instead of vacuum) and liquid phases in equilibrium (or quasi-equilibrium) state:

$$<\beta_\Delta(T)> = <\beta_g(T)> - <\alpha_g(T)>.\tag{3}$$

Note that $\Delta G_{l\to v}>0$, while $\Delta G_{v\to l}<0$.

Simplified approaches to estimating the values of β using the TST are based on the expressions[51]

$$\beta_{V,g}=[1-(V_l/V_g)^{1/3}]\exp(-\Delta G_{ev}/RT),\tag{4}$$

$$\beta_V=[1-(V_l/V_g)^{1/3}]\exp\{-0.5/[(V_g/V_l)^{1/3}-1]\},\tag{5}$$

where V_l and V_g are the specific volumes of the liquid and gas phases, respectively. Subscript V indicates that the expression for β explicitly depends on the specific volumes. The definitions of all

6

constants and coefficients and more detailed description of equations are given in the SI. Averaged (over a set of conformers) values of β ($\langle\beta\rangle$) are also used later in the paper (see SI[58]).

The CDM effects, which can contribute to the Gibbs free energies of evaporation, $\Delta G_{ev}(T)$, and solvation, $\Delta G_s(T)$, were analysed using the MSTor program[62,63] applied to n-dodecane at 300-1200 K. Ninety five stable conformers (see Tables S1-S3 in SI[58]) were selected based on the changes in the Gibbs free energy from 1000 conformers generated by ConfGen[62] and analysed using MSTor.[62,63] Note that the numbers referring to conformers under consideration (see Table S1[58]) are random and do not depend on the value of G (see Tables S2 and S3[58]). This was done to obtain a relatively random set of conformers at various $N \leq 95$ characterised by wide distributions of the values of G. The details of calculations are given in SI[58].

III. RESULTS AND DISCUSSION

There are several sets of factors which are expected to affect the evaporation/condensation processes of n-dodecane droplets. Firstly, these are those linked to structure, population, and transformation of various conformers of n-dodecane in the gas and liquid phases. Secondly, these are those due to features of the surroundings of the molecules at the surface and in the bulk of droplets and those related to orientation of evaporating/condensing molecules and a number of neighbouring molecules at the droplet surface. Thirdly, these are temperature, total and partial gas pressures, liquid and gas densities. Most of these factors will be analysed below using the QC approaches enhanced by empirical or model corrections.

The orientation of relatively long n-dodecane molecules (*e.g.* unbent conformer S1 is approximately 1.6 nm long) at the surfaces of droplets can affect the values of β. This orientation affects a number of neighbours of an evaporating molecule,[40,41] and, therefore, the energy which needs be spent to remove the molecule into the gas phase (or into the interfacial layer) from the droplet

surface. During condensation of *n*-dodecane molecules, the orientation of attacking molecules relative to the droplet surface and molecules at this surface (see Fig. 1a and Fig. S1 in SI[58]) can affect the accommodation coefficient.[40,41]
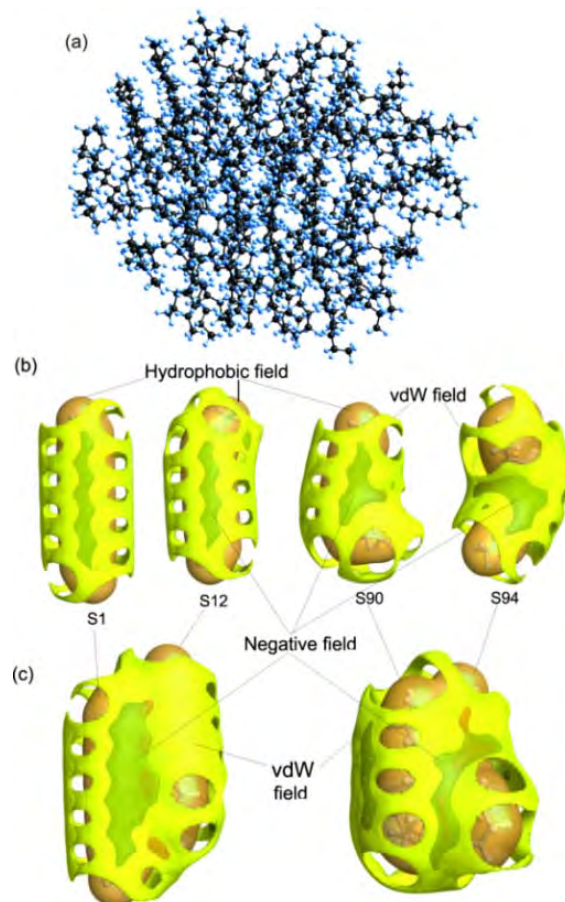

FIG. 1. (a) A nanodroplet (cluster) with 64 *n*-dodecane molecules used in the MD modelling of heating at 293 K for 20 ps and then at 400 K for 20 ps using MM+ FF (VEGA ZZ[64] with NAMD[65]); (b, c) visualisation of the vdW, hydrophobic (describing regions with high hydrophobicity), and negative (due to positive charges on the H atoms) fields around the molecules (calculated using TorchLite[59,60]) for (b) individual conformers (S1, S12, S90, and S94) and (c) conformers merged in dimers S1 & S12 and S90 & S94.

The analysis of these effects within the scope of the TST was based on consideration of corrected surface Gibbs free energy of solvation $w\Delta G_s$ at $w < 1$ instead of ΔG_s (as a measure of ΔG_{ev}) calculated for molecules in the bulk liquid. The correction factor w in $\Delta G_{ev} = \Delta G_{l \to g} = -w\Delta G_s$ was used.[41] Parameter $w < 1$ takes into account that the number of neighbours of an evaporating molecule at a surface is smaller than in the bulk liquid. Using 3D models of droplets,[40,41] one can assume that the

value of *w* can be smaller for bent conformers and is expected to be in the range of $0.25 - 1$. This effect was analysed for several conformers located perpendicular ($w = 1$, the evaporating molecule is located completely inside the droplet) or parallel ($w \approx 5/8$, the evaporating molecule is semi-submerged in the surface layer of the droplet) to the surface of the droplet (Fig. 2).
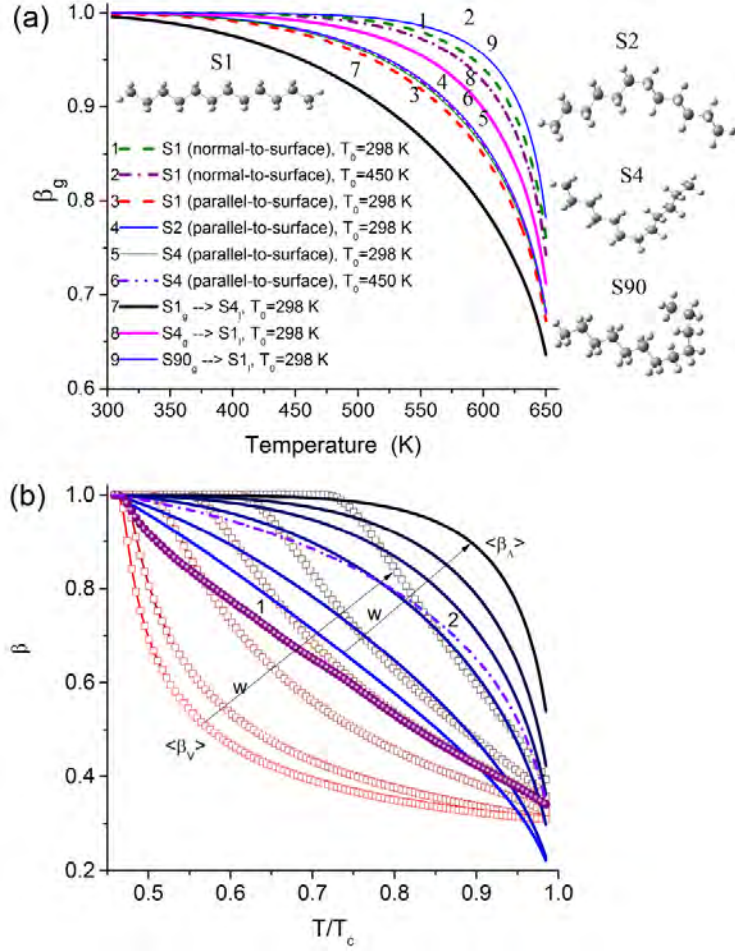

FIG. 2. Condensation coefficient *vs.* temperature: (a) β_g with two orientations of a molecule at the surface of a liquid *n*-dodecane droplet normal to the surface ($w = 1$) or parallel to the surface ($w = 5/8$)[40,41] for conformers S1, S2, S4, and S90. T_0 is the temperature for both phases in QC calculations. (b) Averaged $\langle \beta_\Delta \rangle$ (symbols) and $\langle \beta_V \rangle$ (curves) with CDM at $w = 0.25, 0.3333, 0.5, 0.625, 0.75$ and 1 (arrows correspond to increased values of *w*) and curves calculated based on arithmetic averaging (curves 1 and 2). Calculations were carried out using ωB97X-D/cc-pVTZ and SMD/ωB97X-D/cc-pVTZ for (a) selected conformers and (b) a collection of selected 73 conformers (see Table S2[58]) at pressure of 0.35 MPa.

The MD FF approach can be used for modelling thermal swelling and evaporation of an *n*-dodecane nanodroplet (see Fig. 1a and Fig. S1 in SI[58]). The results based on this approach, as well as previous QC calculations,[40,41] indicate the presence of various orientations of the molecules at the

9

surface, as well as in the gas phase. Also, the molecules in both phases represent an ensemble of various conformers (see Fig. 1b and Table S1 in SI[58]). Strongly bent molecules (*e.g.* conformers S90 and S94 (Fig. 1)) are characterised by vdW and negative fields, different (especially around chain inflection) from those around linear (S1) or slightly bent (S12) ones (Fig. 1b,c). The former are characterised by higher values of the Gibbs free energy G (see Tables S2 and S3) than the latter. Small patches of negative fields (Fig. 1b,c) are attributed to positive charges on the H atoms (small negative charges are on the C atoms). These charges on the H atoms around the bent fragment increase from 0.08-0.09 a.u. in S1 to 0.11-0.12 a.u. in S90 or S94. Note that solvation in the *n*-dodecane medium results in a small increase in the atom charges in *n*-dodecane conformers. The changes in the fields around strongly bent conformers (Fig. 1b,c) can affect intermolecular interactions (Fig. 1c), and, therefore, the evaporation/condensation processes for various conformers.

At $w = 1$ (*i.e.* an evaporating molecule is completely imbedded into the droplet), the process is characterised by greater values of β_g (and smaller values of γ) in comparison with a molecule drifting parallel to the surface (Fig. 2a). The values of $\langle \beta_V \rangle$ and $\langle \beta_\Delta \rangle$ decrease (by two times or more at T/T_c = 0.6-0.8) with decreasing values of w from 1 to $1/2 - 1/4$ (Fig. 2b). However, at higher temperatures ($T/T_c > 0.85$) this effect seemed to be less visible. In our calculations, $w = 5/8$ is used as an average value for surface molecules, since the curves averaged by w (Fig. 2b, curves 1 and 2) are located close to the corresponding curves calculated at $w = 5/8$. Thus, molecules with bent chains and upright portions above the droplet surface plane can be more easily evaporated due to smaller contact area with neighbouring molecules, despite slightly increased polarisation of the bent chain (Fig. 1). This is one of the reasons for enhancement of the evaporation rate and reduction of the values of β due to the CDM effects. It should be noted that a sample ensemble with 73 conformers (used in the calculations with cc-pVTZ, Fig. 2b) is sufficiently wide to study the CDM effects (*vide infra*).

Molecules located in the interfacial layer outside the liquid droplet (see Fig. S1b-e in SI[58]) undergo weak intermolecular interactions with molecules at the droplet surface. The difference in the Gibbs free energies of molecules in the gas phase and the interfacial layer is much smaller than that for the molecules in the gas and liquid phases. Therefore, it is not easy to estimate the values of β for transfer of the molecules between the interfacial layer and the gas phase in terms of the changes in the Gibbs free energy (the value of w should be very small, < 0.1, for the interfacial layer). This could be done within the QC MD modelling,[40,41] and is not studied in our paper.

Note that the formation of vapour bubbles inside bulk liquid at $T \geq T_b \approx 489.5$ K (boiling point of n-dodecane) can enhance the evaporation process. The value of w for molecules evaporated into the bubbles can be greater than that for the molecules evaporated from the outer surface of droplets due to different signs of the surface curvature in these two cases. Therefore, the evaporation from the outer surface of droplets is faster than that into the bubbles. The bubble formation and the contribution of the interfacial layer are not studied in our paper.

Also, the values of β depend on the CDM in both phases and the details of the process of transfer between these phases. If the evaporation occurs without changes in the conformer structure, the orientation effects at the surface are predominant (Fig. 2a).[40,41] If CDM occurs during the transfer process, the value of β_g is lower for condensed conformers having higher Gibbs free energy in the gas phase than in the liquid phase. For example, the value of β_g is lower for $S1_g \rightarrow S4_l$ transfer (see Fig. 2a, curve 7) than that for $S4_g \rightarrow S1_l$ transfer (see Fig. 2a, curve 8) as S1 is a more stable conformer than S4 in both phases (see Tables S2 and S3 in SI[58]). The values of T_0 (298.15 or 450.0 K) for both phases in QC calculations of the Gibbs free energy weakly affect the values of β_g calculated with corrections described by Eq. (S4)[58] (see Fig. 2a, curves 1 and 2 or 5 and 6). Therefore, the main part of the QC calculations was performed at $T_0 = 298.15$ K with the temperature corrections based on Eq. (S4)[58].

The density distribution functions of the changes in the Gibbs free energy during transfer of conformers between the gas and liquid phases or for CDM in the same phase (Fig. 3) can be calculated using the following equation[66]

$$f(\Delta G) = (2\pi\sigma^2)^{-0.5} \sum_{i=1}^{N} \exp[-(\Delta G_i - \Delta G)^2 / 2\sigma^2] ,\qquad(6)$$
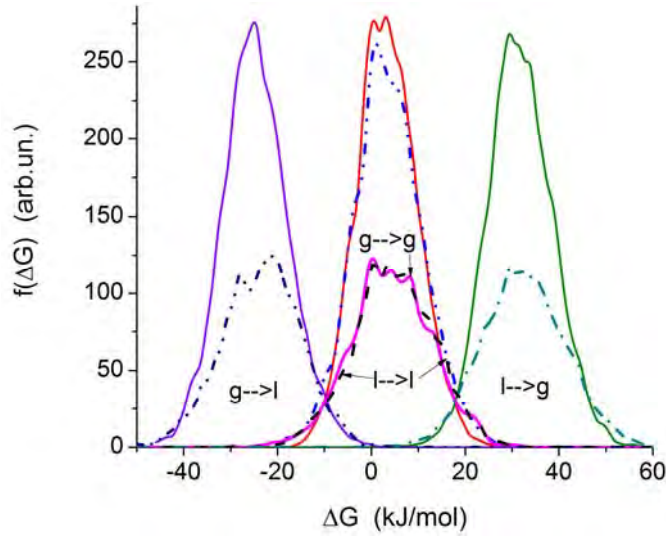
where σ is the distribution variance.

FIG. 3. The Gibbs free energy distribution functions, $f(\Delta G)$ for conformerisation during the transfer between phases $\Delta G_{g \to l}$ and $\Delta G_{l \to g}$ or in the same phase ($\Delta G_{g \to g}$ (solid lines) and $\Delta G_{l \to l}$ (dot-dashed lines) (2)) or, calculated from Eq. (6) at $\sigma =$ 0.5 kJ/mol for 73 conformers (see Table S2[58]) with the cc-pVTZ basis set (lower curves) and 95 conformers with the cc-pVDZ basis set (upper curves)

This function for a smaller ensemble (73 conformers, calculated using cc-pVTZ) has a shape similar to that for a larger ensemble of 95 conformers (cc-pVDZ) (see Fig. 3). However, the latter is characterised by higher peaks due to the larger number of samples in the ensemble. Therefore, the calculations with the larger basis set (cc-pVTZ) were carried out for a smaller ensemble of the conformers than was used in the calculations with the cc-pVDZ basis set.
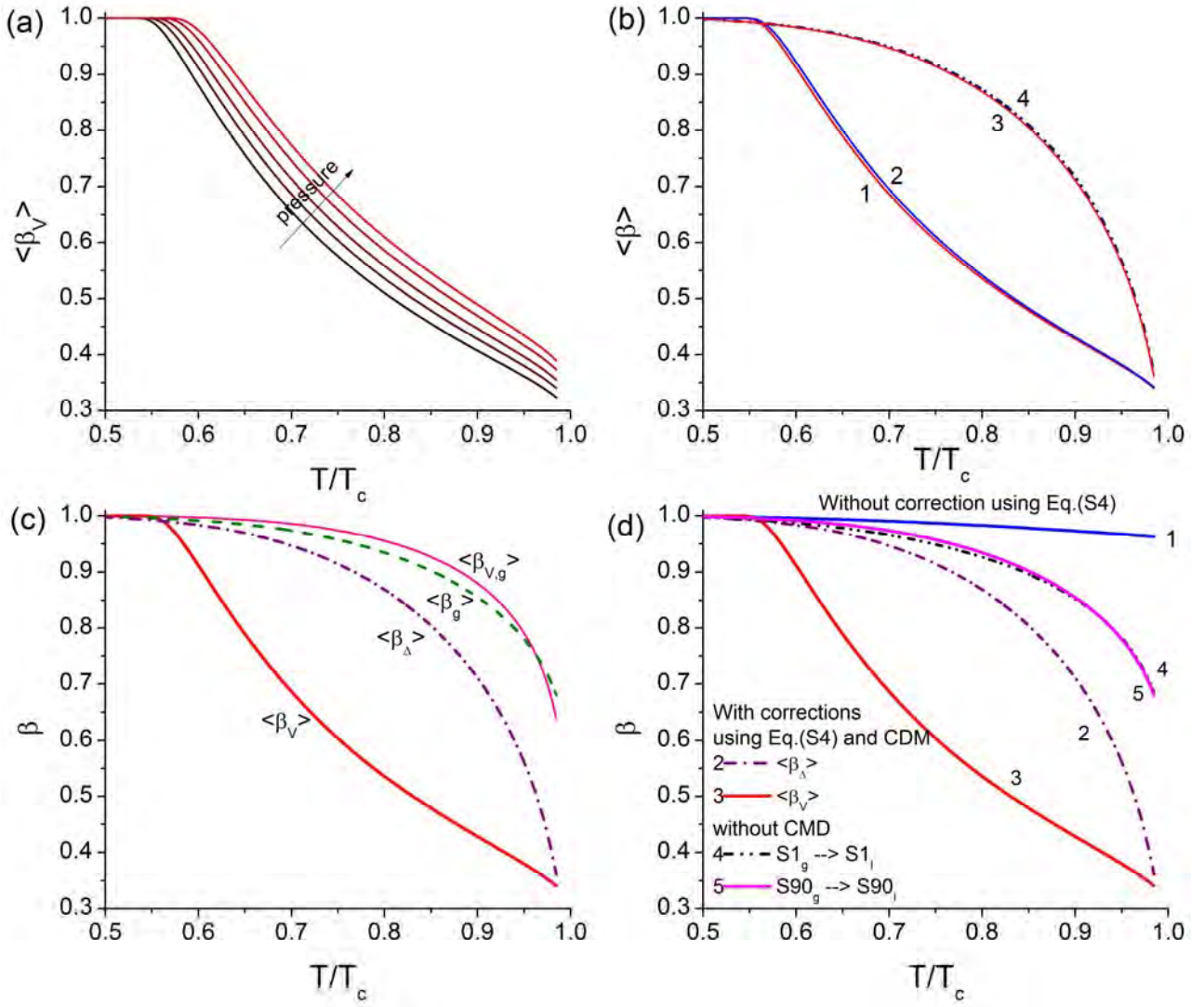
FIG. 4. (a) Effects of pressure (0.1, 0.35, 1, 3.5 and 10 MPa) in the gas phase on the average values of the evaporation/condensation coefficient ($\langle \beta_V \rangle$); (b) $\langle \beta_V \rangle$ (lower curves) and $\langle \beta_\Delta \rangle$ (upper curves) for 73 (curves 1 and 3) and 95 (curves 2 and 4) conformers calculated using cc-pVTZ and cc-pVDZ, respectively; (c) $\langle \beta_V \rangle$, $\langle \beta_{V,g} \rangle$, $\langle \beta_\Delta \rangle$ and $\langle \beta_g \rangle$; and (d) $\langle \beta_g \rangle$ (curve 1) without correction using Eq. (S4),[58] $\langle \beta_\Delta \rangle$ (curve 2) with corrections taking into account the dependence of the vaporisation enthalpy of n-dodecane on temperature and orientation of molecules at a surface of liquid n-dodecane ($\Delta G_{g \to l} = 5/8\ \Delta G_s$ at 298.15 K), $\langle \beta_V \rangle$ (curve 3), curves 4 and 5 refer to corrected β_Δ, but without CDM, for transfers of conformers S1 and S90, respectively. Selected 73 conformers in Figures a-d (see Table S2[58]) calculated with cc-pVTZ by ωB97X-D and SMD/ωB97X-D and 95 conformers in Figure b (see Table S3[58]) were calculated with the cc-pVDZ basis set at (a) various pressures or (b-d) 0.35 MPa.

As mentioned above, pressure in the gas phase affects the value of β. According to QC calculations, using Eqs. (S7) and (S11)[58] and CDM, the average values $\langle \beta_V \rangle$ increase with increasing

pressure (see Fig. 4a). The effects of temperature on $\langle \beta_V \rangle$ at a constant pressure (volume of the gas phase increases with T) and at $p \sim T$ (due to restricted volume of the gas phase) are small. These effects are of the same order of magnitude as those due to CDM.

The effects of the basis sets used (cc-pVTZ or cc-pVDZ) and the number of conformers in the ensembles (73 or 95 conformers) on the values of β are small (Fig. 4b and Fig. S2). Therefore, calculations of β for all 95 conformers were carried out only with the smaller cc-pVDZ basis set, and the larger cc-pVTZ basis set was used for a smaller number of conformers but this set included the conformers with both minimal and maximal values of G in both phases (see Tables S2 and S3 in SI[58]).

The difference between the values of $\langle \beta_V \rangle$ and $\langle \beta_\Delta \rangle$ can be larger (Fig. 4b) than the one which can be attributed to ignoring changes in the n-dodecane density in the gas phase (affecting ΔG) in calculations of the values of $\langle \beta_\Delta \rangle$. In contrast to the calculations of $\langle \beta_\Delta \rangle$, the values of $\langle \beta_V \rangle$ were computed taking into account changes in the density in both phases with temperature which strongly affected the exponential part in Eq. (S8)[58]. The application of Eq. (S7)[58] with the exponential part ignoring changes in the density of n-dodecane in the gas phase gives values of $\langle \beta_{V,g} \rangle$ close to $\langle \beta_g \rangle$ (Fig. 4c). Thus, ignoring the temperature dependence of the n-dodecane density in the gas phase on calculation of the values of $\langle \beta_\Delta \rangle$ with CDM, as well as fixing gas pressure used in calculations of the values of $\langle \beta_V \rangle$ with CDM, can lead to overestimation of the values of $\langle \beta_\Delta \rangle$ and underestimation of the values of $\langle \beta_V \rangle$, since, in the restricted volume, pressure increases with temperature (see Eq. (S9)[58]). This leads to the corresponding increase in $\langle \beta_V \rangle$ (Fig. 4a).

Analysing the influences of temperature, pressure, and gas/liquid density on β, one can anticipate that the application of Eq. (S4)[58] can give better results than direct calculations of the Gibbs free energy of evaporation $\Delta G_{ev}(T) = -\Delta G_s(T)$ based on the SMD method to calculate $\Delta G_s(T)$) at 0.45

14

$< T/T_c < 1.0$.[40,41] The reasons for overestimation of $-\Delta G_s(T)$ in direct SMD calculations at $T > 300$ K

can be linked to underestimation of a decrease in the liquid density with temperature. This can affect

some physical characteristics, including permittivity and polarisability, and cause reduction of short-

range intermolecular vdW and other interactions. The latter are related to increased average distances

between molecules. This leads to overestimation of the values of β (Fig. 4d, curve 1) in comparison

with the corrected values of $\langle \beta_\Delta \rangle$ (Fig. 4d, curve 2), and this difference increases with temperature.

The effect of CDM on the evaporation/condensation processes can be seen from the

comparison of $\langle \beta_\Delta \rangle$ with CDM correction (Fig. 4d, curve 2) and β_Δ without CDM correction (see Fig.

4d, curves 4 and 5). Close results (Fig. 4d, curves 4 and 5) observed for $S1_g \rightarrow S1_l$ (S1 with the ideal

linear structure has low Gibbs free energy) and $S90_g \rightarrow S90_l$ (S90 with a strongly bent structure, see

Fig. 1b and Table S1 in SI[58], has high Gibbs free energy, see Tables S2 and S3[58]) can be explained by

similar solvation effects for these conformers. This closeness leads to closeness in the changes in the

Gibbs free energy during evaporation/condensation and solvation processes (Fig. 3). Thus, the

evaporation/condensation process is expected to be affected by the transformation of conformers. This

effect can be related to the fact that the difference in the Gibbs free energy for various conformers in

the gas and liquid phases can be smaller than that for the same conformers in these two phases. As

follows from our analysis, $\langle \beta_V \rangle < \langle \beta_\Delta \rangle$ in a wide temperature range (see Fig. 4d, curves 2 and 3).

Note that the changes in the gas phase density $vs.$ T and p were taken into account in calculations of

$\langle \beta_V \rangle$, but not those of $\langle \beta_\Delta \rangle$.

MD simulations with various potentials and approaches used to compute β[14,35] give smaller

values than $\langle \beta_g \rangle$ and $\langle \beta_\Delta \rangle$ obtained using QC taking into account the CDM, especially at $T/T_c > 0.7$

(Fig. 5). This can be related to the underestimation of intermolecular interactions in the liquid n-

dodecane, described by the MD FF, and in the gas phase, described by QC, at high temperatures (Fig.

5). The values of $\langle \beta_V \rangle$, computed using QC(TST), taking into account the CDM and changes in the gas phase density, are closer to $\langle \beta_\Delta \rangle$ than those computed using the MD FF for structureless LJ fluids and those computed based on a simplified model of an *n*-dodecane molecule (including United Atom Model). The values of $\langle \beta_V \rangle$ are slightly larger than the latter only at $T/T_c > 0.75$ due to underestimation of intermolecular interactions in the gas phase at high temperatures by MD FF.
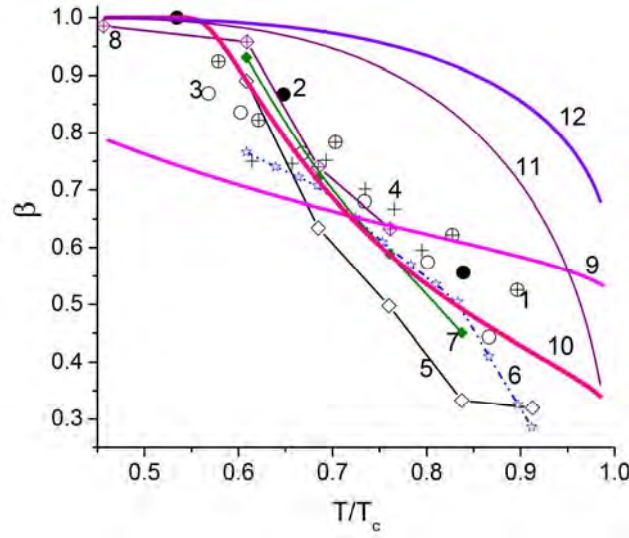
FIG. 5. Comparison of the values of the evaporation coefficient, predicted by MD FF (symbols 1-4, curves 5-8) and QC (curves 9-12) models. Symbols (1-4) refer to the models for structureless LJ fluids with various input parameters,[52] curves 5 and 7 refer to the results obtained based on the united atom model reported in[13] and in[14] respectively, curve 6 refers to the results of calculations based on the TST model reproduced from[13], curve 8 is based on the results of calculations using the model described by Mizuguchi *et al.*[35] The following QC processes were considered: S90$_l$→S1$_g$ (curve 9) with $\Delta G_{l \rightarrow g} =$ 3.3 kJ/mol at $T_0 = 298.15$ K. Also the curves calculated based on the averaging of the contributions of 73 conformers (see Table S2[58]) for $\langle \beta_V \rangle$ (curve 10), $\langle \beta_\Delta \rangle$ (curve 11) and $\langle \beta_g \rangle$ (curve 12) at 0.35 MPa and $w = 5/8$ are presented. QC calculations were performed using ωB97X-D/cc-pVTZ and SMD/ωB97X-D/cc-pVTZ.

$\Delta G_{l \rightarrow g}$ (estimated at $T_0 = 298.15$ K in Eq. (S4)[58]), corresponding to process S90$_l$ → S1$_g$ (see Tables S2 and S3 in SI[58]), makes a relatively small contribution to the evaporation of *n*-dodecane since conformer S90 has ΔG_s higher than that of S1 by 23.7 kJ/mol. Therefore, the population of S90 conformers in liquid and gaseous *n*-dodecane is expected to be small. The same conclusion applies to other conformers with high Gibbs free energy (Fig. 3). The values of $\langle \Delta G_{l \rightarrow g} \rangle$ for all possible transfers for all conformers under consideration are greater than those for S90$_l$ → S1$_g$. The values of

16

$\langle \beta_{\mathrm{g}} \rangle$ and $\langle \beta_{\Delta} \rangle$ at $T/T_{\mathrm{c}} > 0.65$ are greater than $\langle \beta_{\mathrm{V}} \rangle$ or those calculated using the MD FF methods (Fig. 5a).[6,8,14]

The CDM effect on β decreases with increasing temperature (Fig. 5). The CDM effects on the changes in the values of β are similar to those due to pressure (Fig. 4a). However, at temperatures close to T_{c} the pressure effects are stronger than those of the CDM.

A decrease in the intermolecular vdW interaction energy with temperature due to reduction of the liquid density results in a decrease in the values of β. The increase in the vdW interaction energy (related to the size of evaporated molecules or increase in the number of neighbours, see Fig. 2b) leads to a decrease in the values of γ.[40,41] Similar results were obtained for evaporating dimers[41] and trimers of molecules. The CDM effects leading to decreasing in β (see Figs. 4 and 5) cause increasing in the evaporation rate (Fig. 6, curve 2) and decreasing in the evaporation time (Fig. 6, curve 4) in comparison with those computed without consideration of the CDM effects (see Fig. 6, curves 1 and 3). These effects are attributed to reduction in the interactions of the evaporating molecules with neighbours and favourable changes in the Gibbs free energy of evaporation of certain conformers during their transfer into the gas phase.
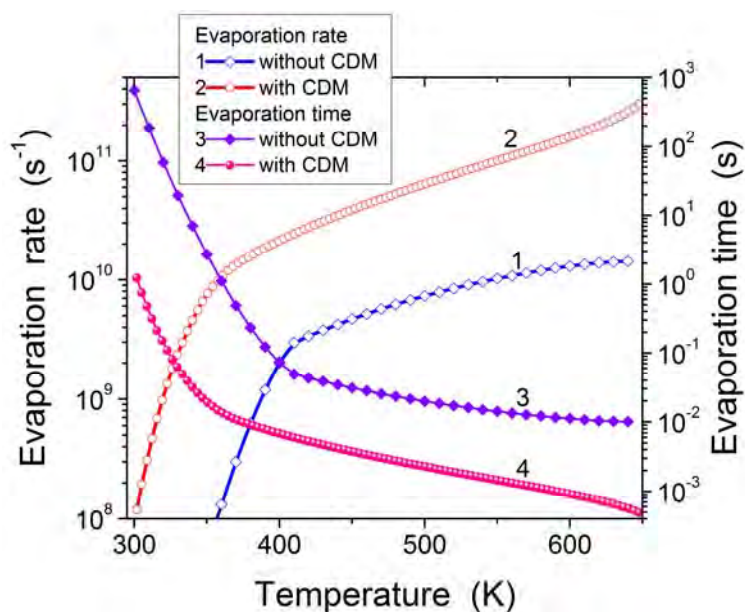
FIG. 6. Comparison of the evaporation rate γ (curves 1 and 2) and evaporation time (curves 3 and 4) of an *n*-dodecane microdroplet (droplet radius 2.65 μm with number of molecules 1.46×10^8 and pressure 3.5 MPa) not taking CDM into account (curves 1 and 3) and taking CDM into account (curves 2 and 4). 73 conformers (see Table S2[58]) calculated using ωB97X-D/cc-pVTZ and SMD/ωB97X-D/cc-pVTZ were studied.

IV. CONCLUSION

The conformation-dependent evaporation/condensation processes of *n*-dodecane have been studied using quantum chemical DFT (functional ωB97X-D with the cc-pVTZ and cc-pVDZ basis sets) and SMD methods. Zero-point and thermal corrections to the Gibbs free energy in the gas phase and additional solvation terms for the molecules in the liquid phase have been taken into account. The geometry of 95 conformers has been optimised using ωB97X-D/cc-pVTZ. The transition state theory (TST) has been applied to estimate the values of the evaporation/condensation coefficient. It is shown that the effects of conformerisation/cross-conformerisation and changes in the surroundings (number of adjacent molecules at a droplet surface) of evaporating molecules, as well as temperature, pressure, and gas and liquid density, play important roles in the evaporation/condensation processes of *n*-dodecane. The range of changes in the Gibbs free energy of small ensembles of selected conformers is shown to be more important than the numbers of conformers in the ensembles. This allows us to focus our analysis on only two conformers with maximal and minimal values of *G* in both phases. The

18

predicted values of β *vs*. temperature are expected to be close to those inferred from the analysis of all 95 conformers. Changes in the interactions of evaporating molecules with the surroundings in the surface layer of a droplet are shown to affect β more strongly than the conformerisation and cross-conformerisation of the molecules in the gas and liquid phases or pressure in the gas phase. Also, the CDM effects are shown to be maximal at $T/T_c = 0.6\text{-}0.7$ and decrease with decreasing or increasing temperatures. They become negligible at $T/T_c < 0.55$ or T/T_c close to 1.

To enhance the reliability of the approach developed in our study, corrections to be applied in the analysis of the changes in the Gibbs free energy of evaporating/condensing molecules are suggested. These corrections are based on (i) the tabulated (experimental) data for the temperature dependence of the evaporation enthalpy and the density of the gas and liquid phases of *n*-dodecane, and (ii) the differences in the surroundings of molecules at a droplet surface and in bulk liquid. The approach developed in our paper gives values of β which are close to β calculated for structureless LJ fluids and to β calculated for *n*-dodecane using MD FF methods, except at temperatures close to the critical temperatures.

[1]   M. A. Silberberg, *Chemistry – The Molecular Nature of Matter and Change,* Fourth edition (McGraw-Hill, New York, 2006).

[2]   *Handbook of Atomization and Sprays,* edited by V. Ashgriz (Springer, Heidelberg, 2011).

[3]   S. Fujikawa, T. Yano, and M. Watanabe, *Vapor-Liquid Interfaces, Bubbles and Droplets* (Springer, Heidelberg, 2011).

[4]   M. B. McElroy, *The Atmospheric Environment* (Princeton University Press, Princeton, 2002).

[5]   *Evaporation, Condensation and Heat Transfer,* edited by A. Ahsan (InTech, Rijeka, Croatia, 2010).

[6]   S. S. Sazhin, *Droplets and Sprays* (Springer, London, 2014).

[7] S. Chapman and T. G. Cowling, *The Mathematical Theory of Nonuniform Gases* (Cambridge University Press, Cambridge, 1970).

[8] S. S. Sazhin, *Progr. Energy Combus. Sci.* **32**, 162 (2006).

[9] J. Tamim and W. L. H. Hallett, *Chem. Eng. Sci.* **50**, 2933 (1995).

[10] A. M. Lippert and R. D. Reitz, *SAE Technical Paper* 972882 (1997).

[11] W. L. H. Hallett, *Combus. Flame* **121,** 334 (2000).

[12] G.-S. Zhu and R. D. Reitz, *Int. J. Heat Mass Transf.* **45,** 495 (2002).

[13] B.-Y. Cao, J.-F. Xie, and S. S. Sazhin, *J. Chem. Phys.* **134**, 164309 (2011).

[14] J.-F. Xie, S. S. Sazhin, and B.-Y. Cao, *Phys. Fluids* **23**, 112104 (2011).

[15] S. S. Sazhin, M. Al Qubeissi, R. Nasiri, V. M. Gun'ko, A. E. Elwardany, F. Lemoine, F. Grisch, and M. R. Heikal, *Fuel* **129**, 238 (2014).

[16] H. Yanagihara, I. Stanković, F. Blomgren, A. Rosén, and I. Sakata, *Combust. Flame* **161**, 541 (2014).

[17] S. Cheng, J. B. Lechman, S. J. Plimpton, and G. S. Grest, *J. Chem. Phys.* **134**, 224704 (2011).

[18] M. S. Hanchak, M. D. Vangsness, L. W. Byrd, and J. S. Ervin, *Int. J. Heat Mass Transf.* **75**, 196 (2014).

[19] M. Knott, H. Vehkamäki, and I. J. Ford, *J. Chem. Phys.* **112**, 5393 (2000).

[20] H. W. Hu and G. H. Tang, *Appl. Therm. Eng.* **62**, 671 (2014).

[21] S.-M. Kim and I. Mudawar, *Int. J. Heat Mass Transf.* **77**, 627 (2014).

[22] A. Lotfi, J. Vrabec, and J. Fischer, *Int. J. Heat Mass Transf.* **73**, 303 (2014).

[23] I. J. Ford and S. A. Harris, *J. Chem. Phys.* **120**, 4428 (2004).

[24] P. Sosnowski, A. Petronio, and V. Armenio, *Int. J. Heat Mass Transf.* **66**, 382 (2013).

[25] L. Yang, X. Quan, P. Cheng, and Z. Cheng, *Int. J. Heat Mass Transf.* **78**, 460 (2014).

[26] M. E. Vieira da Silva, K. Schwarzer, B. Hoffschmidt, F. P. Rodrigues, T. Schwarzer, and P. A. Costa Rocha, *Renew. Energy* **53**, 174 (2013).

[27] S. Natarajan, S. A. Harris, and I. J. Ford, *J. Chem. Phys.* **124**, 044318 (2006).

[28] X. Lv and B. Bai, *Appl. Therm. Eng.* **65**, 24 (2014).

[29] B. Peng, W. He, X. Hao, Y. Chen, and Y. Liu, *Comput. Mater. Sci.* **87**, 260 (2014).

[30] S. Takata and F. Golse, *Eur. J. Mech. - B/Fluids* **26**, 105 (2007).

[31] M. Bond and H. Struchtrup, *Phys. Rev. E* **70**, 061605 (2004).

[32] V. K. Badam, V. Kumar, F. Durst, and K. Danov, *Exp. Therm. Fluid Sci.* **32**, 276 (2007).

[33] W. S. Drisdell, C. D. Cappa, J. D. Smith, R. J. Saykally, and R. C. Cohen, *Atmos. Chem. Phys.* **8**, 6699 (2008).

[34] M. Zientara, D. Jakubczyk, K. Kolwas, and M. Kolwas, *J. Phys. Chem. A* **112**, 5152 (2008).

[35] H. Mizuguchi, G. Nagayama, and T. Tsuruta, *Seventh International Conference on Flow Dynamics* (Sendai, Japan, 2010, p. 386).

[36] J.-F. Xie, S. S. Sazhin, I. N. Shishkova, and B.-Y. Cao, *Proc. International Symposium on Advances in Computational Heat Transfer* (1-6 July, 2012 Bath, UK, CD, Begell House Inc., paper CHT12-MP02, 2012).

[37] J.-F. Xie, S. S. Sazhin, and B.-Y. Cao, *J. Thermal Sci. Technol.* **7**, 288 (2012).

[38] I. K. Ortega, O. Kupiainen, T. Kurtén, T. Olenius, O. Wilkman, M. J. McGrath, V. Loukonen, and H. Vehkamäki, *Atmos. Chem. Phys.* **12**, 225 (2012).

[39] O. Kupiainen, I. K. Ortega, T. Kurtén, and H. Vehkamäki, *Atmos. Chem. Phys.* **12,** 3591 (2012).

[40] V. M. Gun'ko, R. Nasiri, S. S. Sazhin, F. Lemoine, and F. Grisch, *Fluid Phase Equilibria* **356**, 146 (2013).

[41] V. M. Gun'ko, R. Nasiri, and S. S. Sazhin, *Fluid Phase Equilibria* **366**, 99 (2014).

[42] C.A. Hunter, *Chem. Sci.* **4**, 834 (2013).

[43] *Encyclopedia of Computational Chemistry,* edited by P. v. R. Schleyer (John Wiley & Sons, New York, 1998).

[44] P. W. Atkins and R. Friedman, *Molecular Quantum Mechanics*, Fourth edition (Oxford University Press, Oxford, 2005).

[45] COSMOthermX, Version C30_1301, December 12th, (COSMOlogic GmbH & Co. KG, Leverkusen, Germany, 2012).

[46] Y. Fujitani, K. Saitoh, A. Fushimi, K. Takahashi, S. Hasegawa, K. Tanabe, S. Kobayashi, A. Furuyama, S. Hirano, and A. Takami, *Atmospheric Environment* **59**, 389 (2012).

[47] S. Dirbude, V. Eswaran, and A. Kushari, *Atomization and Sprays* **21**, 787 (2011).

[48] G. Guéna, C. Poulard, and A. M. Cazabat, *Colloids Surf. A: Physicochem. Eng. Aspects* **298**, 2 (2007).

[49] M. Heldmann, T. Knorsch, and M. Wensing, *SAE Int. J. Engines* **6**, 1213 (2013).

[50] L. Zigan, I. Schmitz, A. Flügel, M. Wensing, and A. Leipertz, *Fuel* **90,** 348 (2011).

[51] G. Nagayama and T. Tsuruta, *J. Chem. Phys.* **118**, 1392 (2003).

[52] A. Lotfi, J. Vrabec, and J. Fischer, *Int. J. Heat Mass Transf.* **73**, 303 (2014).

[53] M. J. Frisch, G. W. Trucks, H. B. Schlegel, G. E. Scuseria, M. A. Robb, J. R. Cheeseman, G. Scalmani, V. Barone, B. Mennucci, G. A. Petersson, H. Nakatsuji, M. Caricato, X. Li, H. P. Hratchian, A. F. Izmaylov, J. Bloino, G. Zheng, J. L. Sonnenberg, M. Hada, M. Ehara, K. Toyota, R. Fukuda, J. Hasegawa, M. Ishida, T. Nakajima, Y. Honda, O. Kitao, H. Nakai, T. Vreven, J. A. Montgomery, Jr., J. E. Peralta, F. Ogliaro, M. Bearpark, J. J. Heyd, E. Brothers, K. N. Kudin, V. N. Staroverov, T. Keith, R. Kobayashi, J. Normand, K. Raghavachari, A. Rendell, J. C. Burant, S. S. Iyengar, J. Tomasi, M. Cossi, N. Rega, J. M. Millam, M. Klene, J. E. Knox, J. B. Cross, V. Bakken, C. Adamo, J. Jaramillo, R. Gomperts, R. E. Stratmann, O. Yazyev, A. J. Austin, R. Cammi, C. Pomelli, J. W. Ochterski, R. L. Martin, K. Morokuma, V. G. Zakrzewski, G. A. Voth, P. Salvador, J. J. Dannenberg, S. Dapprich, A. D. Daniels, O. Farkas, J. B. Foresman, J. V. Ortiz, J. Cioslowski, and D. J. Fox, *Gaussian 09*, Revision D.01 (Gaussian, Inc., Wallingford CT, 2013).

[54]   J.-D. Chai and M. Head-Gordon, *Phys. Chem. Chem. Phys.* **10,** 6615 (2008).

[55]   K. Yang, J. Zheng, Y. Zhao, and D. G. Truhlar, *J. Chem. Phys*. **132**, 164117 (2010).

[56]   A.V. Marenich, C.J. Cramer, and D.G. Truhlar, *J. Phys. Chem. B* **113,** 6378 (2009).

[57]   A. D. Becke, *J. Chem. Phys.* **140**, 18A301 (2014).

[58]   Supplementary Material Document No._____ describing calculation models, some calculation results, and structures of 95 conformers of *n*-dodecane.

[59]   T. Cheeseright, M. Mackey, S. Rose, and J. G. Vinter, *Expert Opin. Drug Discov*. **2,** 131 (2007).

[60]   T. Cheeseright, M. Mackey, S. Rose, and J. G. Vinter, *J. Chem. Inf. Model.* **46**, 665 (2006).

[61]   G.A. Zhurko and, D.A. Zhurko, Chemcraft (version 1.7, build 382), 2014, http://www.chemcraftprog.com.

[62]   J. Zheng, S. L. Mielke, K. L. Clarkson, and D. G. Truhlar, *Comp. Phys. Comm*. **183**, 1803 (2012).

[63]   J. Zheng, R. Meana-Pañeda, and D. G. Truhlar, *Comp. Phys. Comm.* **184**, 2032 (2013).

[64]   A. Pedretti, L. Villa, and G. Vistoli, *J. Comput.-Aided Mol. Des*. **18**, 167 (2004).

[65]   J. C. Phillips, R. Braun, W. Wang, J. Gumbart, E. Tajkhorshid, E. Villa, C. Chipot, R. D. Skeel, L. Kale, and K. Schulten, *J. Comput. Chem.* **26**, 1781 (2005).

[66]   V. M. Gun'ko and V. V. Turov, *Nuclear Magnetic Resonance Studies of Interfacial Phenomena* (CRC Press, Boca Raton, 2013).

Supplementary Information

Effects of the surroundings and conformerisation of *n*-dodecane molecules on evaporation/condensation processes

Vladimir M. Gun'ko

Chuiko Institute of Surface Chemistry, 17 General Naumov Street, Kiev 03164, Ukraine and
Sir Harry Ricardo Laboratories, School of Computing, Engineering and Mathematics, University of Brighton,
Cockcroft Building, Lewes Road, Brighton BN2 4GJ, United Kingdom

Rasoul Nasiri and Sergei S. Sazhin

Sir Harry Ricardo Laboratories, School of Computing, Engineering and Mathematics, University of Brighton,
Cockcroft Building, Lewes Road, Brighton BN2 4GJ, United Kingdom

The CDM effects, which can contribute to the Gibbs free energies of evaporation, $\Delta G_{ev}(T)$, and solvation, $\Delta G_s(T)$, were analysed using the MSTor program[1,2] applied to *n*-dodecane at 300-1200 K. Ninety five stable conformers (see Tables S1-S3) were selected based on the changes in the Gibbs free energy from 1000 conformers generated by ConfGen[61] and analysed using MSTor.[1,2] Note that the numbers referring to conformers under consideration (see Table S1) are random and do not depend on the value of G (see Tables S2 and S3). This was done to obtain a relatively random set of conformers at various $N \leq 95$, characterised by wide distributions of the values of G.

The effect of conformerisation of *n*-dodecane molecules resulted in conformation-dependent changes in the Gibbs free energy of the molecules in both phases. The Gibbs free energy of the ensemble of conformers was determined by the formula[3]

$$G_N = -RT \ln \sum_{j=1}^{N} \exp(-G_j / k_B T), \qquad (S1)$$

where N is the number of conformers, R is the universal gas constant, k_B is the Boltzmann constant, and T is the temperature. This equation was applied to conformer ensembles in both gas and liquid phases. The average changes in the Gibbs free energy upon evaporation (or condensation) of a molecule were estimated as

$$\left\langle \Delta G_{l \to g} \right\rangle = (G_{N,g} - G_{N,l}) / N, \tag{S2}$$

where subscripts $_l$ and $_g$ refer to molecules in the liquid and gas phase.

For simplicity, one can assume that the Gibbs free energy of evaporation $\Delta G_{ev} \approx \Delta G_{l \to g}$.[4,5] The evaporation enthalpy ($Q_{ev}(T) > 0$) contributing to $\Delta G_{ev}(T)$ can be estimated for liquid n-dodecane as[6]

$$Q_{ev}(T) = q(1 - T / T_c)^m, \tag{S3}$$

where $q = 77.1658$ kJ/mol and $m = 0.407$ are the equation constants, and $T_c = 658.2$ K is the critical temperature for n-dodecane. Using Eq. (S3), one can estimate changes in ΔG_{ev} as[4,5]

$$\Delta G_{ev}(T) = \left\langle \Delta G_{l \to g}(T_0) \right\rangle Q_{ev}(T) / Q_{ev}(T_0), \tag{S4}$$

where $\Delta G_{l \to g} = -\Delta G_s = G_g - G_l$, $T_0 = 298.15$ K. The estimation of $\Delta G_{ev}(T)$ based on Eq. (S4) is more reliable than direct QC calculation of $\Delta G_{ev}(T)$ at high temperatures,[4,5] using ωB97X-D/cc-pVTZ and SMD/ωB97X-D/cc-pVTZ. Eq. (S4) can slightly overestimate a decrease in ΔG_{ev} with temperature due to different changes in the entropy with temperature for different conformers in the gas and liquid phases. For example, conformer S1 is characterised by small relative changes in the entropy with temperature: $\Delta\Delta S_{g \to l,298K} - \Delta\Delta S_{g \to l,450K} = -0.0028$ kJ mol^{-1} K^{-1} based on calculations using ωB97X-D/cc-pVTZ and SMD/ωB97X-D/cc-pVTZ at 298.15 K and 450 K. There is a similarity in changes in the entropy with temperature for the same conformer in the gas and liquid phases, despite the fact that $\Delta S_g > \Delta S_l$. Thus, the temperature dependence of the Gibbs free energy of evaporation of each conformer is controlled mainly by changes in the enthalpy. Therefore, one can assume that Eq. (S4) can be used for calculations of all conformers considered in our study, despite a certain increase in the entropy contribution into the Gibbs free energy due to the CDM during the transfer of the molecules between the liquid and gas phases.

There is a qualitative agreement between the values of β (or related parameters, $e.g.$ γ[4,5,7,8]) $vs.$ temperature computed using various MD FF approaches,[9-16] transition state theory (TST),[17,18] and

other methods[4,5,7,8,19] and those estimated from experimental data.[17] Scatter in the values of β obtained using various methods for the same compound at the same conditions typically increases with increasing temperature. This can be caused by low-temperature calibration of some parameters used in theoretical methods, which are applied to the analysis of evaporation/condensation at much higher temperatures. To avoid this problem, certain correction factors based on the experimental data have been used.[4-6]

The condensation coefficient, β_g, which is close to the evaporation coefficient for the systems in equilibrium or quasi-equilibrium state, can be estimated in terms of thermodynamic potentials[17,20,21]

$$\frac{1-\beta_g}{\beta_g} = \exp\left(\frac{\Delta G_{v \to l}}{RT}\right). \qquad (S5)$$

where $\Delta G_{v \to l} = G_l - G_v$ is the difference between the Gibbs free energies of molecules in liquid and vacuum. Some limitations of a similar approach based on the transition state theory (TST), *e.g.* related to the energy parameters characterising condensation, were discussed previously.[17,20,21] Our analysis is based on a similar approach. Here, more accurate calculation of Gibbs free energies was used taking into account conformerisation effects and changes in the densities of both phases and the evaporation enthalpy with temperature (*vide infra*). Note that condensation of nonpolar alkane molecules occurs almost without the energy barrier; therefore, we do not focus on the activation free energy in our study. The changes in the Gibbs free energy $\Delta G_{g \to l}$ in Eq. (S5) are estimated using QC methods.[4,5,7,8]

The values of ΔG used in Eqs. (S1) and (S5) were calculated from the corresponding sums of electronic and thermal free energies for selected conformers in the vacuum and liquid phases (adding the terms related to the solvation effects) using QC DFT and SMD methods (see Tables S1-S3). The geometry of all conformers (see Table S1) was optimised using ωB97X-D/cc-pVTZ. To correct function $\beta_g(T)$ taking into account the contribution of the gas phase, one can assume that the fraction

of molecules evaporated into a vacuum to produce the gas phase is determined by the following equation

$$\frac{1-\alpha_g}{\alpha_g} = \exp\left(\frac{\Delta G_{l\to v}}{RT}\right). \tag{S6}$$

where $\Delta G_{l\to v}$ is the change in the Gibbs free energy upon transfer of a molecule from a liquid state into a vacuum to form the gas phase from an evaporated liquid. The value of α_g should be subtracted from β_g to consider the transfer between gas (instead of vacuum) and liquid phases: $\beta_\Delta(T) = \beta_g(T) - \alpha_g(T)$; $\beta_\Delta(T)$ is the condensation/evaporation coefficient in equilibrium between the liquid and gas phases.

Simplified approaches to estimate the values of β using the TST are based on the expressions[21]

$$\beta_{V,g} = [1 - (V_l/V_g)^{1/3}]\exp(-\Delta G_{ev}/RT) \tag{S7}$$

$$\beta_V = [1 - (V_l/V_g)^{1/3}]\exp\{-0.5/[(V_g/V_l)^{1/3} - 1]\}, \tag{S8}$$

where V_l and V_g are the specific volumes of the liquid and gas phases, respectively. In Eq. (S7), changes in the gas density *vs. T* are ignored in the exponential term. Subscript V indicates that the expression for β explicitly depends on the specific volumes. The ratio V_l/V_g was computed from the corrected ratio (*vide infra*) of the liquid density[2] and the gas density using the equation of state for real gases[22]

$$p = \rho RT\left[1 + \delta\left(\frac{\partial A}{\partial \delta}\right)_\tau\right], \tag{S9}$$

where p is the pressure, $\tau = T_c/T$, $\delta = \rho/\rho_c$, ρ and $\rho_c = 1.33$ mol/dm^3 are the density and critical density of *n*-dodecane, respectively, and A is the Helmholtz free energy:[22]

$$A(\delta,\tau) = \delta(n_1\tau^{0.32} + n_2\tau^{1.23} + n_3\tau^{1.5}) + \delta^2[n_4\tau^{1.4} + n_5\delta\tau^{0.07} + n_6\delta^5\tau^{0.8} + n_7\tau^{2.16}\exp(-\delta)] +$$
$$n_8\delta^5\tau^{1.1}\exp(-\delta) + \delta\exp(-\delta^2)(n_9\tau^{4.1} + n_{10}\delta^3\tau^{5.6}) + \delta^3\exp(-\delta^3)(n_{11}\tau^{14.5} + n_{12}\delta\tau^{12})$$
,

with constants n_1, n_2,...n_{12} given in Table S4. Nonlinear equation (S9) was solved numerically for the gas density of n-dodecane. The density of liquid n-dodecane (ρ_l) vs. temperature was calculated from the following expression[6]

$$\rho_l(T) = ab^{-(1-T/T_c)^n} ,$$ (S10)

where $a = 0.2344$, $b = 0.25231$, and $n = 0.2896$ are constants.

To estimate the specific volume ratios in Eqs. (S7) and (S8), we need to take into account that gas density depends on the amount of evaporated conformers:

$$\frac{V_l}{V_g} = \frac{\rho_g}{\rho_l} \exp\frac{\langle\Delta G_{g\rightarrow l}\rangle}{RT} ,$$ (S11)

Substitution of Eq. (S11) into Eq. (S8), gives the expression for the evaporation coefficient taking into account the CDM effects. In this case, the expression for the condensation coefficient averaged over the states of various conformers transferred between two phases can be presented as:

$$\langle\beta_V\rangle = \left\{1 - \left[\frac{\rho_g}{\rho_l}\exp\frac{\langle\Delta G_{g\rightarrow l}\rangle}{RT}\right]^{1/3}\right\}\exp\left\{-0.5\left[\left[\frac{\rho_g}{\rho_l}\exp\frac{\langle\Delta G_{g\rightarrow l}\rangle}{RT}\right]^{-1/3}-1\right]^{-1}\right\}.$$ (S12)

where the brackets in $\langle\beta_V\rangle$ indicate the above-mentioned averaging.

Also, β_g described by Eq. (S5) was re-written for average $\langle\beta_g\rangle$ taking into account the transfers of various conformers (Eqs. (S1) and (S2))

$$\frac{1-\langle\beta_g\rangle}{\langle\beta_g\rangle} = \exp\frac{\langle\Delta G_{v\rightarrow l}\rangle}{RT} .$$ (S13)

A similar equation was written for the average correction, $\langle\alpha_g\rangle$, and then for average corrected evaporation coefficient $\langle\beta_\Delta\rangle = \langle\beta_g\rangle - \langle\alpha_g\rangle$. Eq. (S7) was re-written taking into account transfers of various conformers between two phases

5

$$\langle \beta_{V,g} \rangle = \left\{ 1 - \left[\frac{\rho_g}{\rho_l} \exp \frac{\langle \Delta G_{g \to l} \rangle}{RT} \right]^{1/3} \right\} \exp \frac{\langle \Delta G_{g \to l} \rangle}{RT} . \qquad (S14)$$

The equation for the averaged (by states of N conformers) evaporation rate $\langle \gamma_{i(i+j)} \rangle^{4,5,7,8}$ of the ith-molecule (which can be in a different conformer state) from the jth cluster or nano- or micro-droplet (hereafter referred to as droplets), taking into account CDM effects, can be re-written in the form:

$$\langle \gamma_{i(i+j)} \rangle = b_{ij} \frac{p}{k_B T n_0} \exp \frac{\langle \Delta G_{g \to l} \rangle}{RT} , \qquad (S15)$$

where b_{ij} is the collision rate of the ith molecule with the jth droplet calculated using the kinetic gas theory,[4,5,7,8] n_0 is the initial number of molecules in a droplet, p is the reference pressure. For simplicity, the Gibbs free energy of a microdroplet with a very large n_0 ($n_0 \approx 1.46 \times 10^8$ in a microdroplet of radius 2.65 μm is considered in our analysis) is assumed to be unaffected by the removal of a single molecule. The CDM is assumed to take place not only in a certain phase but also during possible changes in conformer states during the transfer of molecules from liquid to gas phase and *vice versa.* This effect depends on the population of states of various conformers in both phases and can affect the values of β and γ *vs*. temperature and pressure.

The geometries of 95 *n*-dodecane conformers optimised using the ωB97X-D/cc-pVTZ method[23] are shown in Table S1. The sums of electronic and thermal free energies for these conformers in the gas and liquid (dodecane medium) phases are shown in Tables S2 (cc-pVTZ) and S3 (cc-pVDZ).

Table S1. Conformers of *n*-dodecane (visualisation is performed using ChemCraft 1.7/382[24]).

S1

S2

S3

S4

S5

S6

S7

S8

S9

S10

S11

S12

S13

S14

S15

S16

S17

S18

S19

S20

S21

S22

S24

7

S23

S25

S26

S27

S28

S29

S30
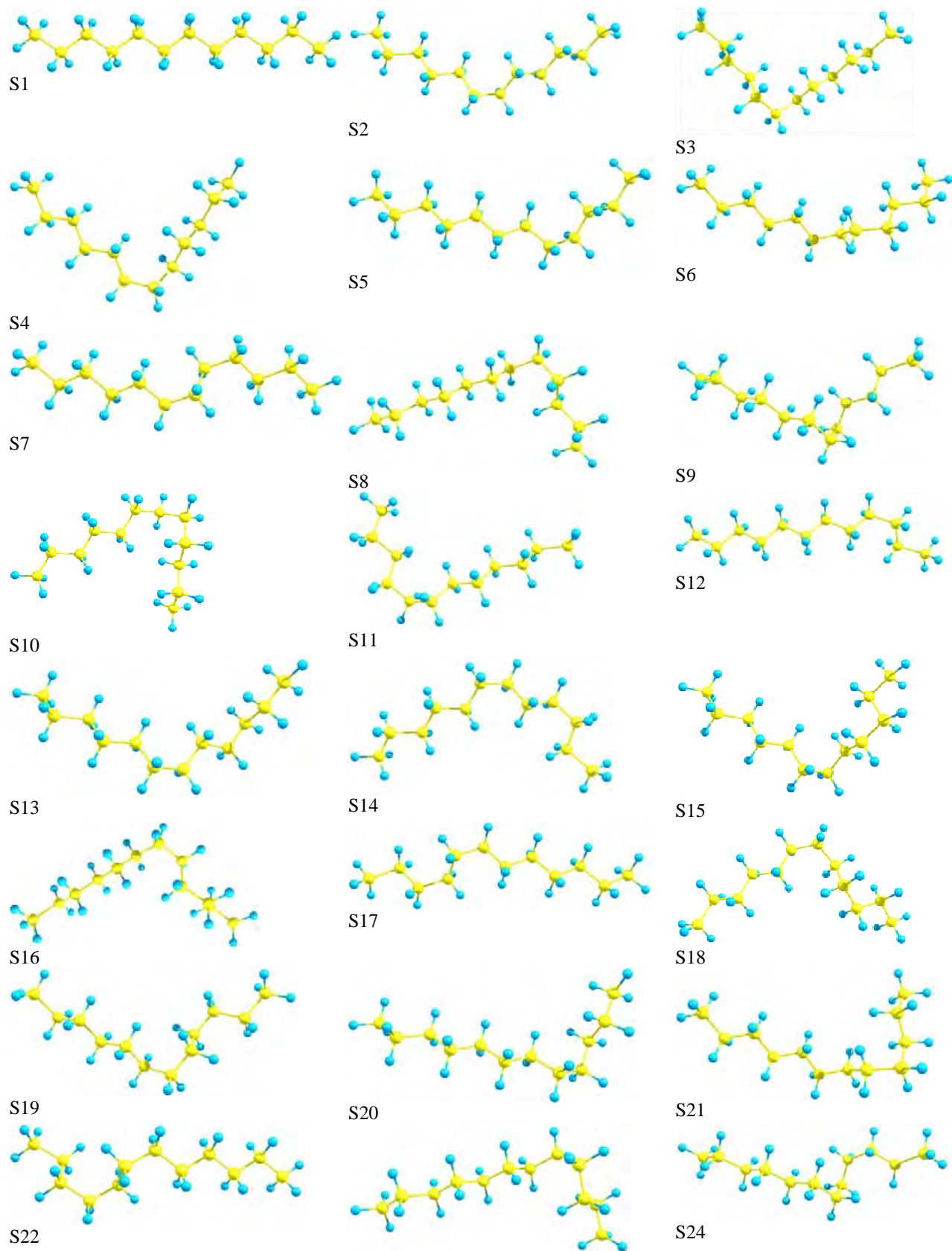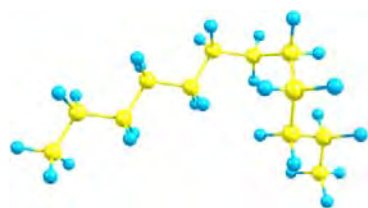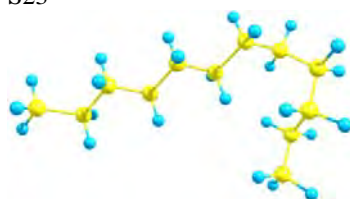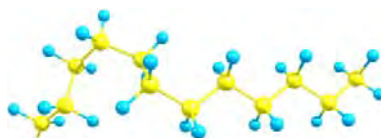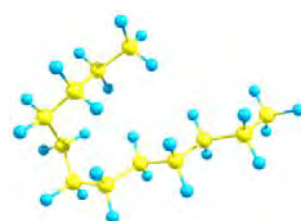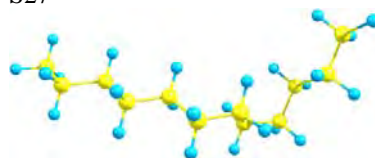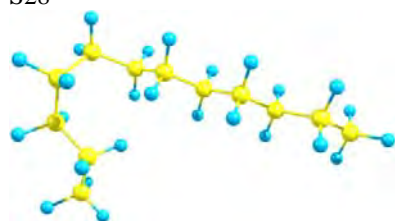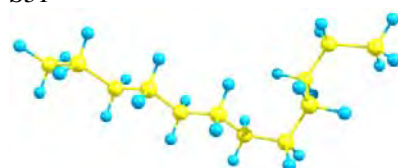
S31
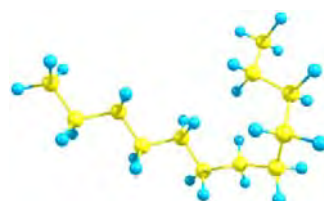
S32
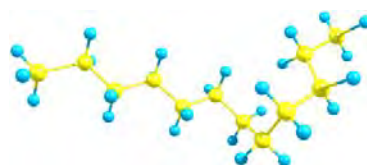
S33
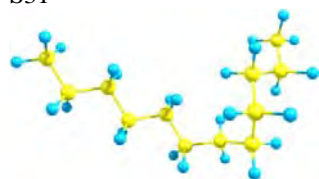
S34

S35
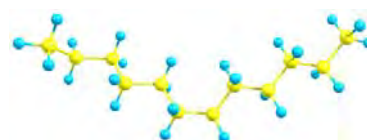
S36
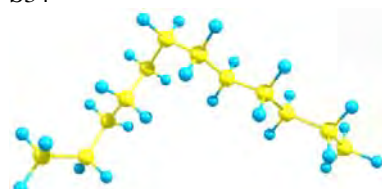
S37
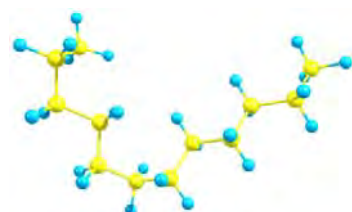
S38
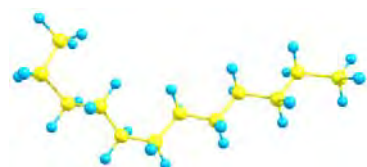
S39
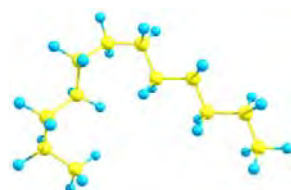
S40

S41

S42

S43

S44

S45

8
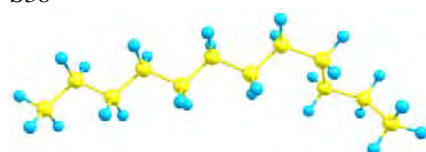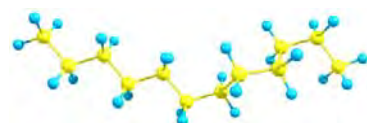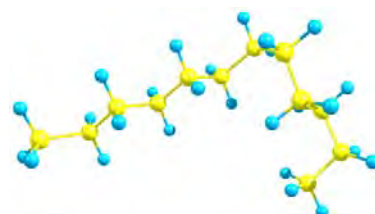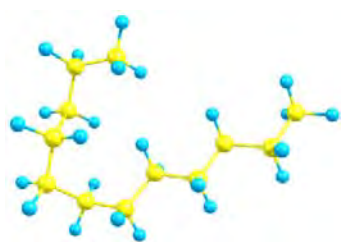
S46
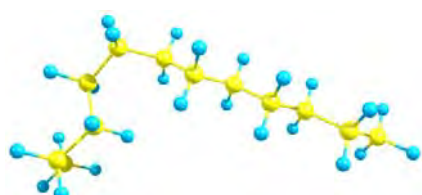
S47
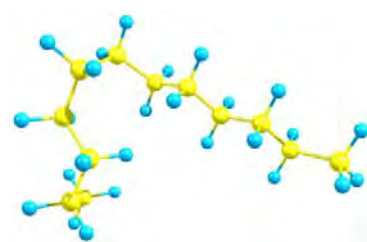
S48

S49

S50
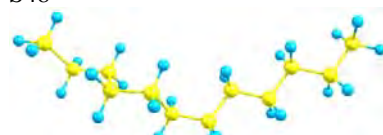
S51
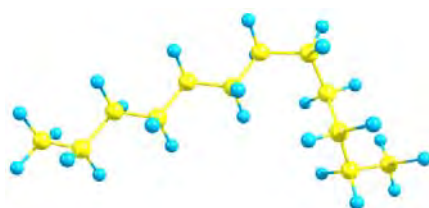
S52

S53

S54

S55
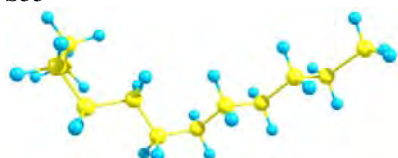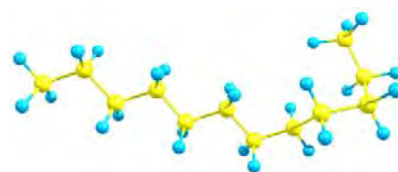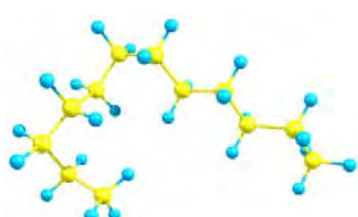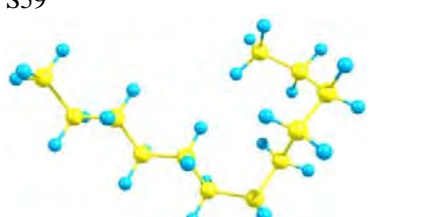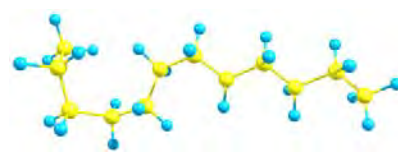
S56
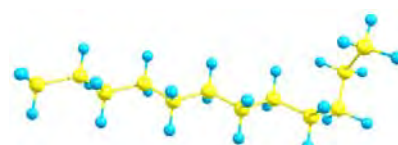
S57
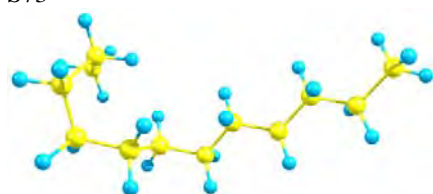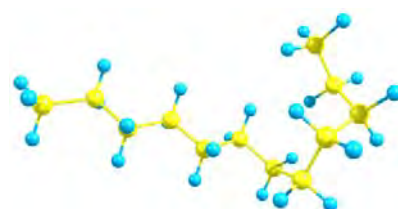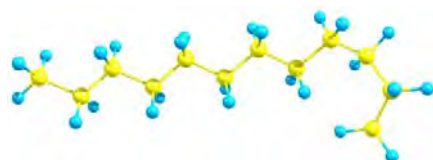
S58

S59

S60

S61

S62

S63

S64

S65

S66

9
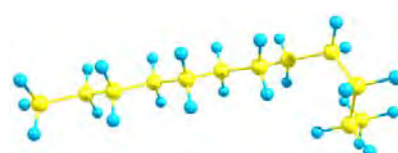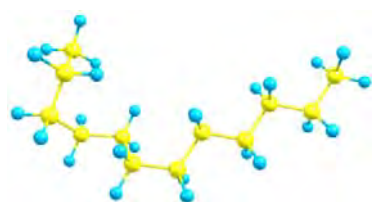
S67
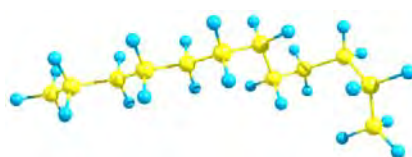
S68

S69
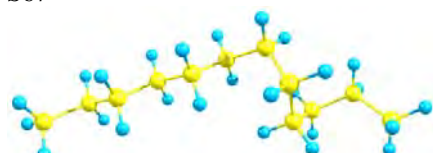
S70
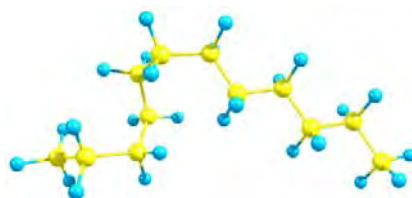
S71

S72

S73

S74

S75

S76

S77

S78

S79

S80

S81

S82
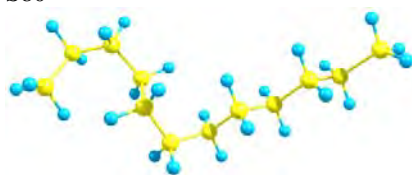
S83
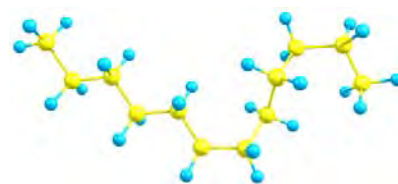
S84
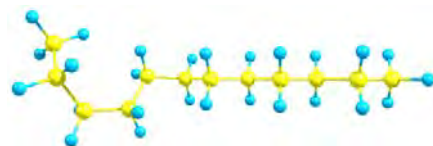
S85
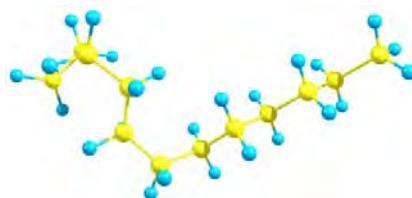
S86

S87
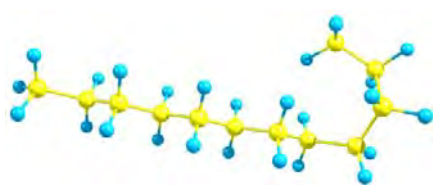
S88
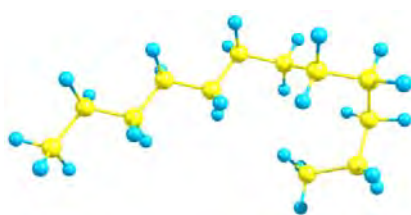
S89

S90

S91

S92

S93

S94

S95

Table S2. Sum of electronic and thermal free energies for *n*-dodecane conformers in the gas (ωB97X-D/cc-pVTZ) and liquid (SMD/ωB97X-D/cc-pVTZ) phases.

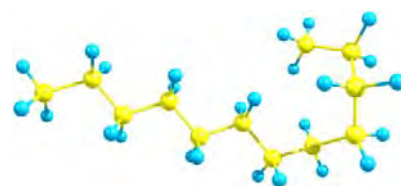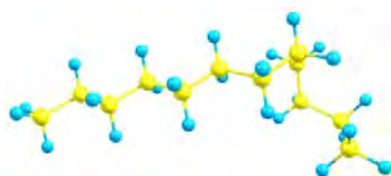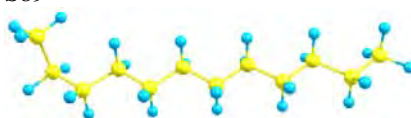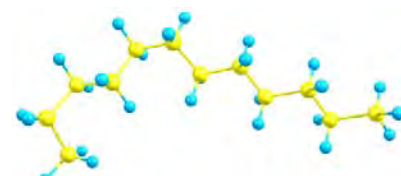| Conformer	Free energy, gas (Ha)	Free energy, liquid (Ha)	Conformer	Free energy, gas (Ha)	Free energy, liquid (Ha)	Conformer	Free energy, gas (Ha)	Free energy, liquid (Ha)
1	-472.672861	-472.683897	33	-472.666819	-472.677786	65		
2	-472.671955	-472.683668	34	-472.667748	-472.678665	66		
3	-472.673521	-472.684762	35	-472.675919	-472.683376	67	-472.670459	-472.679261
4	-472.669991	-472.681439	36	-472.671182	-472.682571	68		
5	-472.673067	-472.685107	37	-472.671964	-472.681410	69	-472.670770	-472.679867
6	-472.671544	-472.683589	38	-472.668438	-472.679998	70		
7	-472.672687	-472.680659	39	-472.671322	-472.682050	71		
8	-472.672774	-472.684828	40	-472.669002	-472.680389	72	-472.669850	-472.680589
9	-472.673212	-472.686184	41	-472.671980	-472.683730	73		
10	-472.669906	-472.681049	42	-472.670167	-472.679637	74		
11	-472.669804	-472.679133	43	-472.673422	-472.680413	75	-472.666560	-472.677692
12	-472.675212	-472.685893	44	-472.672426	-472.680146	76	-472.666759	-472.678866
13	-472.672504	-472.681944	45	-472.671954	-472.682834	77		
14	-472.671916	-472.683465	46	-472.669203	-472.679901	78	-472.667880	-472.678390
15	-472.671710	-472.682647	47	-472.669624		79		
16	-472.670279	-472.679715	48			80	-472.666489	-472.677570
17	-472.669692	-472.681345	49	-472.672894	-472.683414	81	-472.669385	-472.677278
18	-472.667835	-472.678967	50			82		
19	-472.669889	-472.680603	51	-472.668302	-472.679393	83	-472.666826	-472.677891
20	-472.671695	-472.684512	52			84	-472.663619	-472.674752
21	-472.672225	-472.683415	53	-472.668599	-472.680286	85	-472.668170	-472.677190
22	-472.668706	-472.679769	54			86	-472.664836	-472.676118
23	-472.671085	-472.682521	55	-472.670226	-472.677905	87	-472.667376	-472.678708
24	-472.669610	-472.680499	56	-472.671101	-472.680866	88	-472.667298	-472.678691
25	-472.667748	-472.678665	57			89		
26	-472.670753	-472.679134	58	-472.672047	-472.682414	90	-472.664286	-472.674884
27	-472.668744	-472.681313	59			91		
28	-472.669767	-472.681307	60			92	-472.671255	-472.683714
29	-472.666725	-472.677911	61	-472.672385	-472.684404	93		
30	-472.670599	-472.677483	62			94	-472.664719	-472.675590
31	-472.669418	-472.680500	63			95	-472.666980	-472.678400
32	-472.664644	-472.676310	64	-472.668540	-472.679033			

Table S3. Sum of electronic and thermal free energies for *n*-dodecane conformers in the gas (ωB97X-D/cc-pVDZ) and liquid (SMD/ωB97X-D/cc-pVDZ) phases.

Conformer	Free energy, gas (Ha)	Free energy, liquid (Ha)	Conformer	Free energy, gas (Ha)	Free energy, liquid (Ha)	Conformer	Free energy, gas (Ha)	Free energy, liquid (Ha)
1	-472.523718	-472.536180	33	-472.520183	-472.530974	65	-472.521258	-472.531988
2	-472.524363	-472.536351	34	-472.520227	-472.530733	66	-472.521092	-472.535909
3	-472.524183	-472.534954	35	-472.522014	-472.533605	67	-472.523290	-472.531588
4	-472.520231	-472.533893	36	-472.522860	-472.533491	68	-472.520088	-472.530932
5	-472.524272	-472.535570	37	-472.520817	-472.531709	69	-472.520157	-472.531259
6	-472.522554	-472.533916	38	-472.518704	-472.529637	70	-472.521681	-472.533326
7	-472.521138	-472.531907	39	-472.520834	-472.531253	71	-472.519173	-472.529417
8	-472.523033	-472.533925	40	-472.519083	-472.530369	72	-472.520002	-472.530391
9	-472.521465	-472.532437	41	-472.522361	-472.532853	73	-472.519311	-472.528971
10	-472.521094	-472.531911	42	-472.521709	-472.531024	74	-472.519075	-472.533321
11	-472.522214	-472.532445	43	-472.520703	-472.531837	75	-472.519283	-472.530435
12	-472.525748	-472.535872	44	-472.521838	-472.531726	76	-472.517149	-472.528536
13	-472.522719	-472.534085	45	-472.520625	-472.531331	77	-472.518441	-472.530409
14	-472.521392	-472.532285	46	-472.519323	-472.532943	78	-472.518025	-472.528077
15	-472.521383	-472.532118	47	-472.519468	-472.529485	79	-472.519426	-472.530537
16	-472.518722	-472.529702	48	-472.519044	-472.529678	80	-472.517587	-472.528147
17	-472.521900	-472.533374	49	-472.520546	-472.531326	81	-472.519305	-472.529777
18	-472.518747	-472.529494	50	-472.520860	-472.531845	82	-472.520128	-472.530010
19	-472.521103	-472.533524	51	-472.520757	-472.531207	83	-472.516835	-472.527435
20	-472.521806	-472.532981	52	-472.518332	-472.528944	84	-472.515996	-472.526813
21	-472.523320	-472.532183	53	-472.520625	-472.528597	85	-472.518306	-472.529383
22	-472.521439	-472.532268	54	-472.521579	-472.531200	86	-472.517011	-472.527439
23	-472.523563	-472.532066	55	-472.518318	-472.528802	87	-472.517735	-472.528359
24	-472.520825	-472.531337	56	-472.521281	-472.532749	88	-472.521096	-472.531650
25	-472.520227	-472.530733	57	-472.521579	-472.532758	89	-472.521096	-472.531650
26	-472.520093	-472.530484	58	-472.522345	-472.532352	90	-472.516688	-472.524514
27	-472.520094	-472.529550	59	-472.520709	-472.531497	91	-472.519814	-472.530577
28	-472.521146	-472.532177	60	-472.520944	-472.531976	92	-472.522065	-472.533743
29	-472.519135	-472.529929	61	-472.522680	-472.533734	93	-472.520834	-472.531253
30	-472.518375	-472.529393	62	-472.519506	-472.530722	94	-472.514829	-472.525507
31	-472.522044	-472.530218	63	-472.521182	-472.531012	95	-472.518889	-472.530004
32	-472.517217	-472.526370	64	-472.517774	-472.528187			

TABLE S4. Constants for the Helmholtz free energy (for real gas) of n-dodecane.[22]

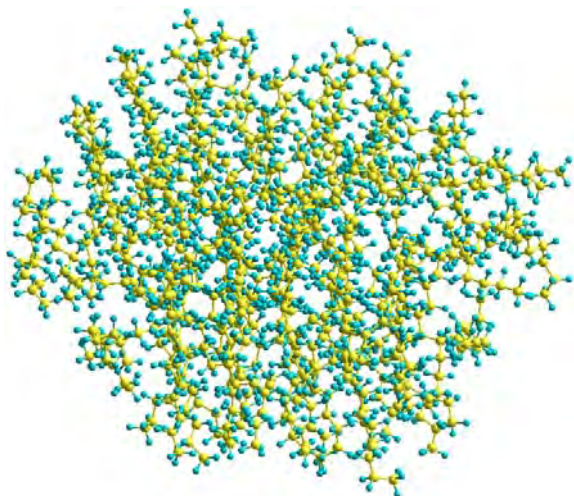| Parameter	Value
n_1	1.38031
n_2	−2.85352
n_3	0.288897
n_4	−0.165993
n_5	0.0923993
n_6	0.000282772
n_7	0.956627
n_8	0.0353076
n_9	−0.445008
n_{10}	−0.118911
n_{11}	−0.0366475
n_{12}	0.0184223

Fig. S1 shows the results of heating of a nanodroplet with 64 molecules of n-dodecane (MD with MM+).
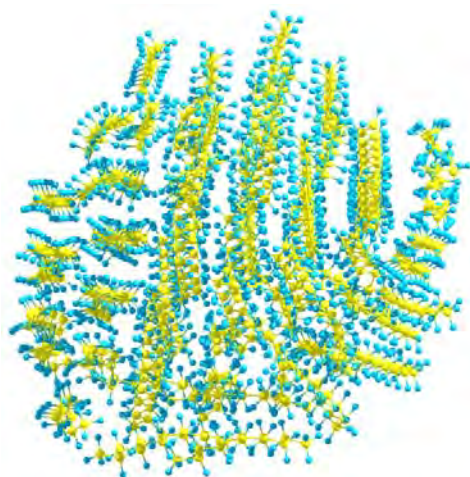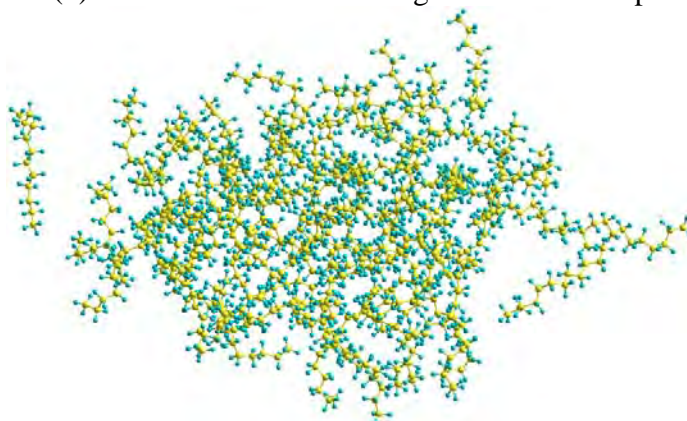

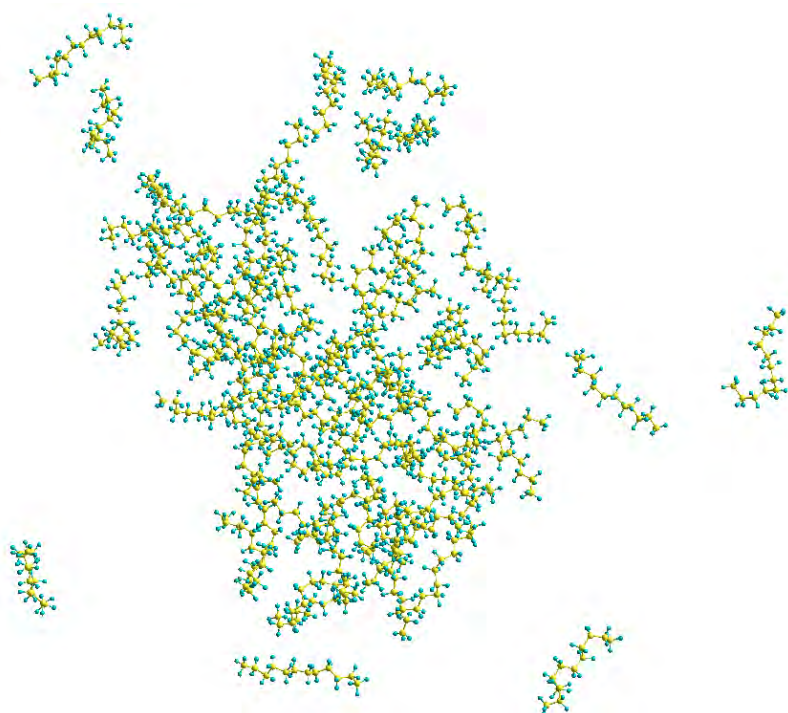(a) Initial structure with unbent molecules
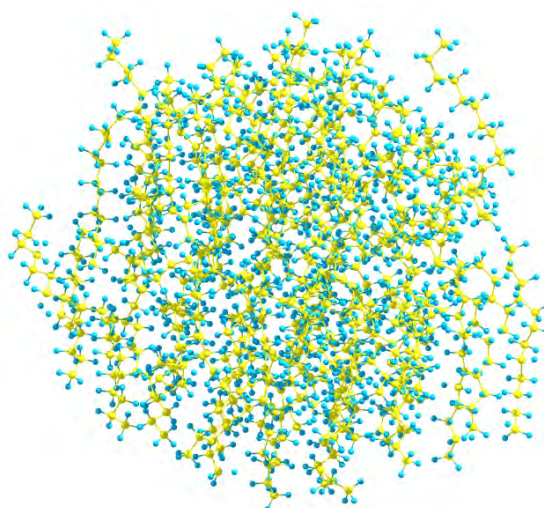
(b) The structure after heating at 293 K for 27 ps

(c)   The structure after subsequent heating at 400 K for 20 ps

(d) The structure after subsequent heating at 489 K for 40 ps

(e) The structure after subsequent heating at 650 K for 20 ps

FIG. S1. The structures of an n-dodecane nanodroplet with 64 molecules predicted by MD with MM+: (a) initial structure, (b)-(e) structures after heating at 293, 400, 489, and 650 K for 27, 40, 20, and 20 ps, respectively (for heating at higher temperature, the structures predicted after heating at lower temperature were used).

The values of $<\beta_V>$ versus normalised temperature, inferred from calculations based on the ωB97X-D/cc-pVTZ method for 73 and 95 conformers, are shown in Fig. S2. As one can see from this figure, the effect of the number of conformers used in calculations (73 and 95) on the values of $<\beta_V>$ is weak and can be safely ignored in practical applications.
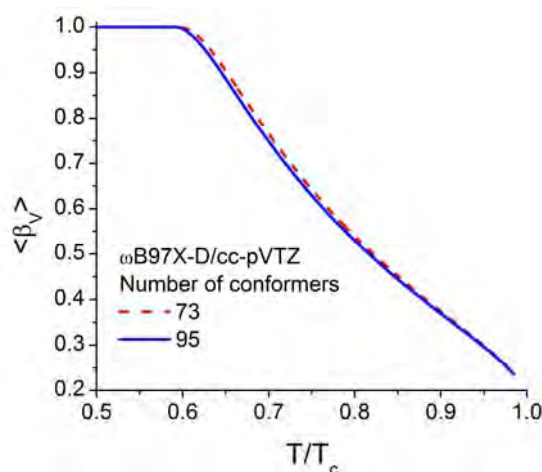
FIG. S2. The effect of the number of conformers (73 and 95) on the values of $\langle\beta_V\rangle$. The calculations were performed using the ωB97X-D/cc-pVTZ method.

1 J. Zheng, S. L. Mielke, K. L. Clarkson, and D. G. Truhlar, *Comp. Phys. Comm*. **183**, 1803 (2012).

2 J. Zheng, R. Meana-Pañeda, and D. G. Truhlar, *Comp. Phys. Comm.* **184**, 2032 (2013).

3 J. Ho, M.L. Coote, C.J. Cramer, D.G. Truhlar, in: Organic Electrochemistry, Fifth Edition, edited by B. Speiser, O. Hammerich (CRC Press, Boca Raton, FL, in press, available at http://comp.chem.umn.edu/Truhlar/docs/C86preprint.pdf).

4 V. M. Gun'ko, R. Nasiri, S. S. Sazhin, F. Lemoine, and F. Grisch, *Fluid Phase Equilibria* **356**, 146 (2013).

5 V. M. Gun'ko, R. Nasiri, and S. S. Sazhin, *Fluid Phase Equilibria* **366**, 99 (2014).

6 *Thermophysical Properties of Chemicals and Hydrocarbons,* edited by C. L. Yaws (William Andrew Inc., Norwich, NY, 2008).

7 I. K. Ortega, O. Kupiainen, T. Kurtén, T. Olenius, O. Wilkman, M. J. McGrath, V. Loukonen, and H. Vehkamäki, *Atmos. Chem. Phys.* **12**, 225 (2012).

8 O. Kupiainen, I. K. Ortega, T. Kurtén, and H. Vehkamäki, *Atmos. Chem. Phys.* **12,** 3591 (2012).

9 S. S. Sazhin, *Droplets and Sprays* (Springer, London, 2014).

10 S. S. Sazhin, *Progr. Energy Combus. Sci.* **32**, 162 (2006).

11 B.-Y. Cao, J.-F. Xie, and S. S. Sazhin, *J. Chem. Phys.* **134**, 164309 (2011).

12 J.-F. Xie, S. S. Sazhin, and B.-Y. Cao, *Phys. Fluids* **23,** 112104 (2011).

13 S. S. Sazhin, M. Al Qubeissi, R. Nasiri, V. M. Gun'ko, A. E. Elwardany, F. Lemoine, F. Grisch, and M. R. Heikal, *Fuel* **129**, 238 (2014).

14 J.-F. Xie, S. S. Sazhin, I. N. Shishkova, and B.-Y. Cao, *Proc. International Symposium on Advances in Computational Heat Transfer* (1-6 July, 2012 Bath, UK, CD, Begell House Inc., paper CHT12-MP02, 2012).

[15] J.-F. Xie, S. S. Sazhin, and B.-Y. Cao, *J. Thermal Sci. Technol.* **7**, 288 (2012).

[16] A. Lotfi, J. Vrabec, and J. Fischer, *Int. J. Heat Mass Transf.* **73**, 303 (2014).

[17] M. Zientara, D. Jakubczyk, K. Kolwas, and M. Kolwas, *J. Phys. Chem. A* **112**, 5152 (2008).

[18] N. M. Laurendeau, *Statistical Thermodynamics: Fundamentals and Applications* (Cambridge University Press, Cambridge, 2005).

[19] COSMOthermX, Version C30_1301, December 12th, (COSMOlogic GmbH & Co. KG, Leverkusen, Germany, 2012).

[20] G. Nathanson, P. Davidovits, D. Worsnop, and C. Kolb, *J. Phys. Chem.* **100**, 13007 (1996).

[21] G. Nagayama and T. Tsuruta, *J. Chem. Phys.* **118**, 1392 (2003).

[22] E. W. Lemmon and M. L. Huber, *Energy & Fuels* **18**, 960 (2004).

[23] M. J. Frisch, G. W. Trucks, H. B. Schlegel, G. E. Scuseria, M. A. Robb, J. R. Cheeseman, G. Scalmani, V. Barone, B. Mennucci, G. A. Petersson, H. Nakatsuji, M. Caricato, X. Li, H. P. Hratchian, A. F. Izmaylov, J. Bloino, G. Zheng, J. L. Sonnenberg, M. Hada, M. Ehara, K. Toyota, R. Fukuda, J. Hasegawa, M. Ishida, T. Nakajima, Y. Honda, O. Kitao, H. Nakai, T. Vreven, J. A. Montgomery, Jr., J. E. Peralta, F. Ogliaro, M. Bearpark, J. J. Heyd, E. Brothers, K. N. Kudin, V. N. Staroverov, T. Keith, R. Kobayashi, J. Normand, K. Raghavachari, A. Rendell, J. C. Burant, S. S. Iyengar, J. Tomasi, M. Cossi, N. Rega, J. M. Millam, M. Klene, J. E. Knox, J. B. Cross, V. Bakken, C. Adamo, J. Jaramillo, R. Gomperts, R. E. Stratmann, O. Yazyev, A. J. Austin, R. Cammi, C. Pomelli, J. W. Ochterski, R. L. Martin, K. Morokuma, V. G. Zakrzewski, G. A. Voth, P. Salvador, J. J. Dannenberg, S. Dapprich, A. D. Daniels, O. Farkas, J. B. Foresman, J. V. Ortiz, J. Cioslowski, and D. J. Fox, *Gaussian 09*, Revision D.01 (Gaussian, Inc., Wallingford CT, 2013).

[24] G.A. Zhurko, D.A. Zhurko, Chemcraft (version 1.7, build 382, 2014), http://www.chemcraftprog.com.